Notes

Photovoltaic Properties of Nano-particulate and Nanorod Array ZnO Electrodes for Dye-Sensitized Solar Cell

Ki Seok Kim, Yoon-Sik Kang, Jung-Hoon Lee, Yu-Ju Shin,* Nam-Gyu Park,† Kwang Sun Ryu,† and Soon Ho Chang†

*Dept. of Chemistry, the Catholic Univ. of Korea, Bucheon, Gyeonggi 422-743, Korea. *E-mail: yujushin@catholic.ac.kr*
†Basic Research Lab., Electronics and Telecommunications Research Institute, Daejeon 305-350, Korea
Received November 18, 2005

Key Words : Nanocrystalline ZnO, Nanorod ZnO, Dye-sensitized solar cell

Grätzel-type dye-sensitized solar cell (DSSC) has been considered as a new candidate for the next solar cell device in the near future.[1,2] Its distinct colorful and transparent features as well as the possibility of low-price production allow much extended applications of DSSC compared to conventional silicon solar cells. Nanocrystalline semiconducting electrode in DSSC, usually made of anatase TiO_2, is the one of essential component of this device, which serves as a supporting transparent film for dye-molecules and then receives the photoelectrons injected from dye-molecules and furnishes them adequate diffusion path to the back-contact. Among various kinds of semiconducting materials with photovoltaic properties,[3-5] anatase TiO_2 has been known as the best due to good matching of conduction band (CB) edge with LUMO level of ruthenium dye-molecule.[6,7]

Considering that CB edge of ZnO has nearly the same energy level with that of TiO_2,[7,8] ZnO should have shown a good photovoltaic performance like TiO_2 or even more enhanced performance, in that ZnO has a wide conduction band originated from the strong covalent interaction of Zn-O through sp^3-hybridization while CB of TiO_2 consists of narrow $\pi^*_{3d\text{-}2p}$ component.[9] Despite such good intrinsic electronic properties of ZnO, however, simple nanocrystalline ZnO electrodes were found to have very poor photovoltaic properties with solar energy conversion efficiency, η < 1% under 1 sun condition,[10,11] and recently reported nanostructured ZnO electrode showed slightly improved values 1.5-3.9%.[12,13] Such low photovoltaic properties of ZnO are mainly related with the unstable surface chemistry of ZnO to acidic dye molecule.[11,14] In this regard, we prepared two kinds of ZnO electrodes, a sintered nano-pariculate electrode and an oriented nanorod electrode and investigated their photovoltaic properties.

Experimental Section

Ethanolic ZnO colloid was prepared by following the method of spanhel and Anderson with some modification.[15,16] After preparing transparent ZnO sol from the reaction of Zn-acetate and $LiOH{\cdot}H_2O$ as described in the literature, the sol was heated at 40 °C for 2 h. As-prepared ZnO nanoparticles were washed with ethanol for 5 times to remove the acetate and hydroxide components. Ethanol solvent was then partially evaporated until ZnO-content became 12 w% and then 4.8 w% of hydroxypropylcellulose (M.W. = 80,000) was added and agitated for 24 h. Nano-particulate ZnO electrode was prepared by casting the paste using a doctor blade on fluorinated SnO_2 conducting glass (TEC8, Pilkington). The thickness of wet film was controlled by using two layers of adhesive tape as a guide between the blade and ZnO paste. The films were heated at 450 ºC under convection for 30 min. and cut into square pieces of 1.5 × 1.5 cm^2 for further uses for DSSC (NPZ). The film thickness of NPZ was found to be 4.2 μm.

The oriented nanorod ZnO electrode was fabricated by crystal-growing method. Nano-particulate ZnO seeds were deposited three times on the fluorinated SnO_2 conducting glass (TEC8, Pilkington) by spin-coating using the colloid prepared above. After each coating of seed, the substrate was dried at 150 ºC for 2-3 h. Nanorods were grown up using those seeded substrates at 92 ºC for 24 h according to the method described by Yang[12,17] and Weller.[18] Aqueous solution of zinc nitrate (0.025 M) and hexamethylenetetraamine (0.025 M) was used for cultivating solution, and refreshed at every 4 h. After reaction, the nanorod array was washed with distilled water and then heated at 400 ºC to get rid of any trace of organic material. The substrate was cut into the same size of nano-particulate ZnO electrode (NRZ). NRZ exhibited a thickness of 3.8 μm, being comparable to NPZ.

Both electrodes were sensitized with 0.5 mM ethanolic solution of ruthenium dye $Ru[dcbpy(TBA)_2]_2(NCS)_2$ (known as N719) for 2 h at 60 ºC. Dye-sensitized semiconducting electrode and Pt-coated counter electrode were assembled with 30-μm thick Surlyn (Dupont) as a spacer. The redox electrolyte solution consisted of 0.6 M 1-hexyl-2,3-dimethyl imidazolium iodide (C6DMI), 0.2 M LiI, 0.04 M I_2 and 0.5 M *tert*-butyl pyridine (TBP) in 3-methoxy propionitrile (MPN)/acetonitrile (ACN) (1 : 1 v/v).

FE-SEM images were obtained using Scanning Electromicroscopy (JEOL, JSM6700F). X-ray diffraction measure-

ment was carried out using Siemens D5005 diffractometer (Cu K_α = 1.5406 Å) equipped with curved graphite monochromator. Photocurrent and voltage were measured employing a Keithley Model 2400 sourcemeter. A small-area solar simulator (PVM, Class B) was used for a light source. The light was homogeneous for small area up to 1 × 1 cm^2 and the intensity was calibrated with a standard single-crystal Si-cell confirmed by NREL.

Results and Discussion

Figure 1 shows FE-SEM photographs of raw ZnO particle, nano-particulate electrode and the nano-rod array and its cross-section. The ZnO particles have a narrow distribution of size 4-6 nm and get fused into bigger grains of 20 nm when heated at 450 °C. The sintered nano-particulate electrode shows a good interconnection of primary particles of ZnO. Nanorod electrode consisted of highly homogeneous nanorod array as shown in Figure 1-(c,d). Hexagonal ZnO rods with aspect ratio *ca*. 15 (length = 3 μm; diameter 200 nm) were grown at a large area scale. The well-defined crystal planes imply that each nanorod of NRZ is almost single crystal and thus NRZ exhibit much higher crystallinity than NPZ which consisted of interconnected nano-particulates. In Figure 2, XRD patterns of raw ZnO powder, NPZ, and NRZ electrodes are represented. NPZ

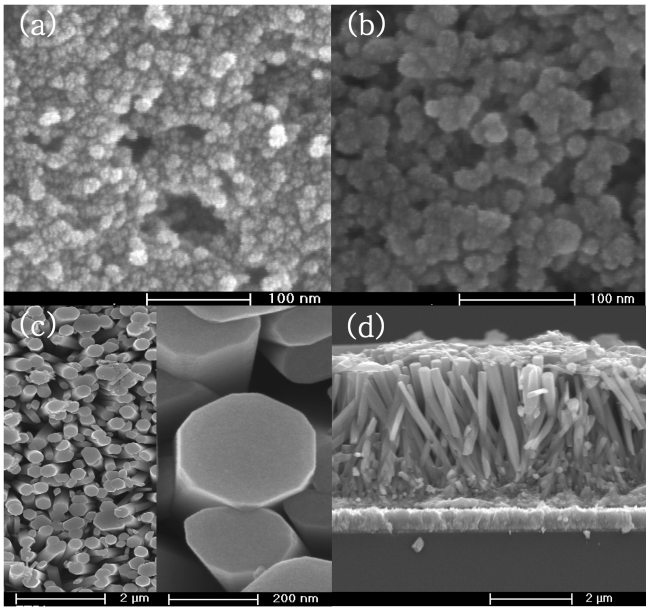

Figure 1. SEM pictures of raw ZnO nanoparticles (a), nano-particulate ZnO electrode (NPZ) (b), nanorod ZnO (NRZ) (c) and its cross-section view (d).

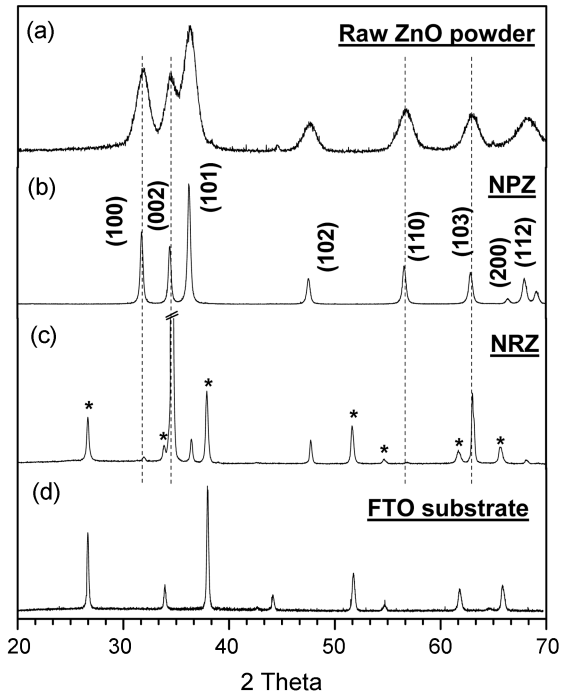

Figure 2. X-ray diffraction patterns of raw ZnO nanoparticles (a), nano-particulate ZnO electrode (NPZ) (b), nanorod ZnO (NRZ) (c) and FTO substrate (d). * denotes the FTO peaks.

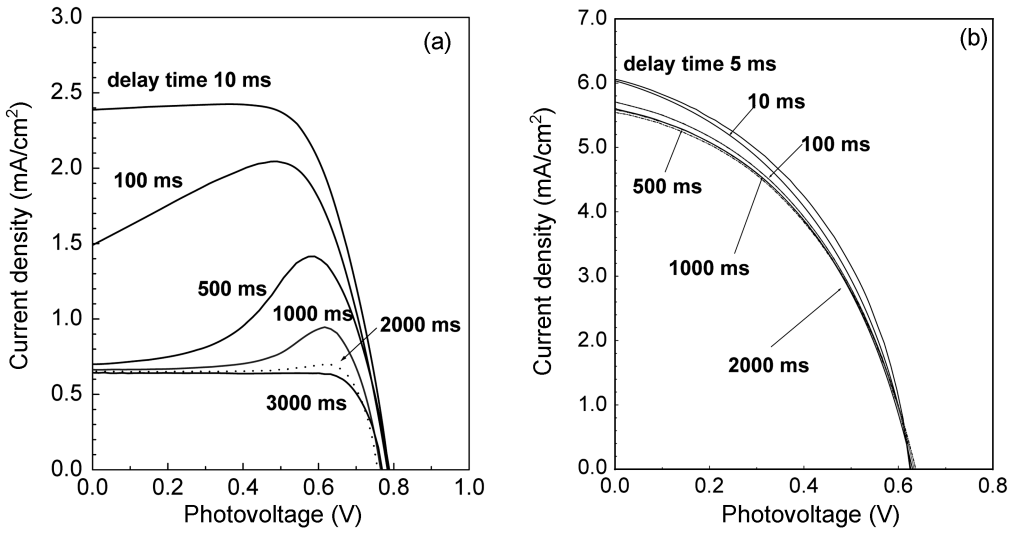

Figure 3. I-V curves at various scan speeds of NPZ (a) and NRZ (b).

Table 1. Photovoltaic properties of ZnO-DSSC under the slow scan condition

Devices	J_{sc} (mA/cm^2)	V_{oc} (V)	fill-factor	η (%)	Delay time	Cell area
NPZ	0.651	0.757	0.89	0.44	3000 ms	0.197 cm^2
NRZ	5.543	0.637	0.44	1.54	2000 ms	0.202 cm^2

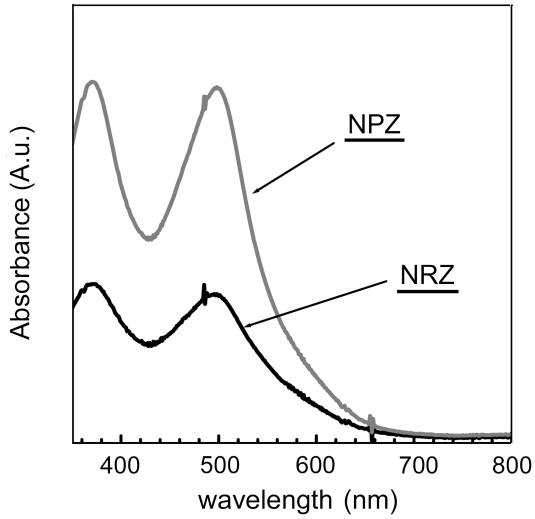

Figure 4. UV-Vis absorption spectra of desorbed dye from the two ZnO electrodes.

exhibited much narrower diffraction lines than raw ZnO powder due to the particle growth as observed in Figure 1. The orientation of nanorods is also reflected in XRD patterns in Figure 2: NRZ shows a XRD pattern in which (002) plane is extremely enhanced, indicating that the ZnO nanorods are well-aligned to the direction of [001].

Figure 3 shows I-V behaviors of two DSSC's, nano-particulate electrode (NPZ) and nanorod electrode (NRZ) and some important photovoltaic properties are listed in Table 1. Measurements were carried out under various scan speed. For each scan, Fifty points of bias voltage from V_{oc} to zero were recorded under various delay-time conditions at 5-3000 ms. I-V response of NPZ was found to be greatly dependant on delay-time. As far as the delay-time is smaller than 2000 ms, I-V curve showed a large variation with scan speed, sometimes showing a hump. In contrast, NRZ exhibited very constant I-V behaviors, even under very short delay-time conditions. The V_{oc} value of NRZ was also kept constant with various measurements compared to NPZ, confirming high device stability NRZ. The adsorption of dye-molecules in the two ZnO electrodes is compared in UV-VIS absorption spectra as presented in Figure 4. NRZ showed much smaller amount of adsorbed dye molecules than NPZ, surely because of small surface area as expected in Figure 1.

The energy conversion efficiency 0.44% found for NPZ is comparable with the studies on similar nano-particulate ZnO electrodes.[10,11] As already mentioned, such a low value can be primarily attributed to the presence of Zn^{2+}-dye aggregates arisen from the unstable surface chemistry of nano-particulate ZnO electrode. During the sensitization, the acidic dye molecules partially dissolve surface ZnO to form Zn^{2+}-dye aggregates which place in nano-pores in electrode and thus to interfere the adequately adsorbed dye-molecules in generating the photoelectrons. At the same time they should also perturb the diffusion of electrolyte I^-/I_3^- throughout the bulk-junction of ZnO electrode/electrolyte by blocking the nanopore channels. Therefore the regeneration of oxidized dye molecules becomes significantly slow down, leading to some retardation of charge transfer. Under this circumstance, the apparent I-V behaviors under rapid scan condition should not be regarded as an inherent property since the performance was not made under a steady-state condition. Such unstable I-V behaviors of NPZ reflect that the diffusion of electrolyte is not so fast to deliver adequately charges for the regeneration of oxidized dye molecules,[19] resulting in a significant reduction of photocurrent. It implies that the generation of photocurrent becomes limited by diffusion of electrolyte.

On the other hand, NRZ exhibited much higher energy conversion efficiency, 1.54% with fill-factor of 0.44. This result is comparable to that of Yang *et al.* (1.5%, ff = 0.38), who explained that this enhanced efficiency is due to the fast electron diffusion within single crystal-like nanorods as confirmed.[12] It was found to be about 100 times faster along a nanorod than through the interconnected ZnO particles. The stable I-V curve of NRZ can be attributed to the presence of very large void spaces between the oriented nanorods. NRZ exhibits large nano-pore channels developed along with the nanorods, Zn^{2+}-dye aggregates are hardly capable to block the diffusion channels and thus the oxidized dye-molecules can be appropriately regenerated. The well-crystallized surface property of nanorods should reduce greatly the formation of Zn^{2+}-dye aggregates.

In summary, the nanorod array ZnO electrode showed stable photovoltaic properties compared with nano-particulate electrode despite the small adsorption of dye-molecules. The well-crystallized surface of nanorod should reduce significantly the formation of Zn^{2+}-dye aggregates. The nanorod array electrode is also favorable for electrolyte diffusion since the diffusion channel is highly spacious and hardly blocked by Zn^{2+}-dye aggregates within the electrode, while the complicated nano-pore channels in nano-particulate electrode can be easily blocked.

Acknowledgement. The authors are grateful for the financial support from ETRI (1010-2005-0091) and KEMCO (2005-N-PV03-P-01).

References

1. O'Regan, B.; Grätzel, M. *Nature* **1991**, *335*, 737.

2. Grätzel, M. *J. Photochem. Photobiol. A: Chem.* **2004**, *164*, 3.
3. Kamat, P. V.; Bedja, I.; Hotchandani, S.; Patterson, L. K. *J. Phys. Chem.* **1996**, *100*, 4900.
4. Chappel, S.; Chen, S. G.; Zaban, A. *Langmuir* **2002**, *18*, 3336.
5. Sayama, K.; Sugihara, H.; Arakawa, H. *Chem. Mater.* **1998**, *10*, 3825.
6. Grätzel, M. *Nature* **2001**, *414*, 338.
7. Xu, Y.; Schoonen, M. A. A. *Amer. Mineralogist* **2000**, *85*, 543.
8. Gao, Y. Q.; Geogievskii, Y.; Marcus, R. A. *J. Chem. Phys.* **2000**, *112*, 3358.
9. Anderson, N. A.; Ai, X.; Lian, T. J. *J. Phys. Chem. B* **2003**, *107*, 14414.
10. Redmond, G.; Fitzmaurize, D.; Grätzel, M. *Chem. Mater.* **1994**, *6*, 686.
11. Bedja, I.; Kama, P. V.; Hua, X.; Lappin, P. G.; Hotchandani, S. *Langmuir* **1997**, *13*, 2398.
12. Law, M.; Greene, L.; Johnson, J. C.; Saykally, R.; Yang, P. *Nature Materials* **2005**, *4*, 455.
13. Hosono, E.; Fujihara, S.; Honma, I.; Zhou, H. *Adv. Materials* **2005**, *17*, 2091.
14. Keis, K.; Lindgren, J.; Lindquist, S.-E.; Hagfeldt, A. *Langmuir* **2000**, *16*, 4688.
15. Spanhel, L.; Anderson, M. *J. Am. Chem. Soc.* **1991**, *113*, 2826.
16. Meulenkamp, E. A. *J. Phys. Chem. B* **1998**, *102*, 2826.
17. Greene, L. E.; Law, M.; Goldberger, J.; Kim, F.; Johnson, J. C.; Zhang, Y.; Saykally, R. J.; Yang, P. *Angew. Chem.* **2003**, *115*, 3139.
18. Pacholski, C.; Kornowski, A.; Weller, H. *Angew. Chem. Int. Ed.* **2002**, *41*, 1188.
19. Koide, N.; Chiba, Y.; Han, L. *Jap. J. Appl. Physics* **2005**, *44*, 4176; Koide, N.; Han, L. *Rev. Sci. Instr.* **2004**, *75*, 2828.